Single-nucleon energies changing with nucleon number

J. P. Schiffer ●,* B. P. Kay ●, and J. Chen ●

Physics Division, Argonne National Laboratory, Lemont, Illinois 60439, USA

Accumulated experimental data on the binding energies for single-particle states in a broad range of nuclei is examined as a function of the constituent number of neutrons and protons and a simple pattern emerges. The dependence of the energies of neutron states on the number of constituent protons, or of proton states on the number of neutrons, behave similar to each other across the nuclear chart, and the sign reflects the well-known strong attraction. The change in energy of neutron states with neutron number or proton states with protons is approximately a factor of four weaker in magnitude and slightly repulsive, except when the changing nucleons are only within the same orbit as the state. These patterns in the experimental data underlie much of what is implicitly understood from nuclear models, but the consistency throughout the periodic table is remarkable.

The representation of the structure of nuclei in terms of the shell model [1,2] was enormously successful over the past approximately 70 years, providing the framework for our understanding. In this approximation nucleons are contained in a mean field in relatively unperturbed single-particle orbits. The mean field is taken to be provided by the rest of the nucleons, and the structure is dependent on the remaining residual effective interaction between the valence nucleons.

The evolution of shell structures in exotic nuclei, the change in the relative energies, and gaps in the energies of single-particle states, was a central theme of the field both experimentally and theoretically, and in particular how they evolve with nucleon number [3,4]. They have provided insights into components of the nucleon-nucleon interaction, such as the role of the tensor force in shell evolution [5] and of three nucleon forces [6,7].

Looking at the absolute changes in these energies, the gross behavior of the binding energy of the last nucleon shows a pronounced difference in how the energies change for valence protons and neutrons, a pattern that was well known [8,9]. For instance, as neutrons fill across the chain of stable, even tin isotopes [10,11], proton states become more bound moving from $A = 112$–124 by about 0.4 MeV per additional neutron, whereas neutron states become less bound over the same range by about 0.1 MeV per neutron. This observation, which reflects the approximately fourfold difference in the magnitudes of the strengths of the np (isospin mixed) and $T = 1$ interactions between nucleons, is apparent simply from the experimentally determined binding energies [12], more commonly referred to as effective single-particle energies.

Here we study these trends more globally, exploring systems across the nuclear chart, taking advantage of the large body of data collected over the past decades. Early attempts

in this direction, notably those of Cohen [13] and Bansal and French [14], observed some of the features, but were focused more narrowly.

The data we consider are presented in Fig. 1, where effective single-particle energies for given j^π orbitals across the nuclear chart, labeled as E_j^π and E_j^ν for protons and neutrons, respectively, are plotted against proton or neutron number Z or N. The data are organized into two categories: (a) showing the evolution of the effective single-particle energies for protons (neutrons) where the neutron (proton) number is changing, reflecting the np interaction, and (b) tracking the effective single-particle energies for protons (neutrons) where the proton (neutron) number is changing, yielding insight into the $T = 1$ interaction.

The data used in compiling Fig. 1 are from specific papers and from compilations, such as Ref. [15]. For example, more detailed work and analyses on transfer reaction data sets on different chains of isotones and isotopes, that provide the necessary information for determining effective single-particle energies are in Refs. [10,11,16–20]. Specific details of the orbitals in Fig. 1 are given in the Supplemental Material [21]. In total, effective single-particle energies for 33 different orbitals, in nuclei from $A = 16$–208 were used, with each segment containing consecutive even-even nuclei. Most of the data included in Fig. 1 are for nominally spherical nuclei, with one exception (labeled ν[521]), where transfer data were obtained on a given orbit across 13 well-deformed rare-earth nuclei [24,25].

In total, 33 segments of single-particle energies were used, a total of about 200 points. In some cases, the energies of the likely dominant component of a state is known, but the strength of the nucleon adding or removing reaction is not, and assumptions were made. In others, there are several measurements that do not quite agree. Most of these differences are consistent with the uncertainties shown in the estimated errors in the figures and do not significantly impact the general features discussed here.
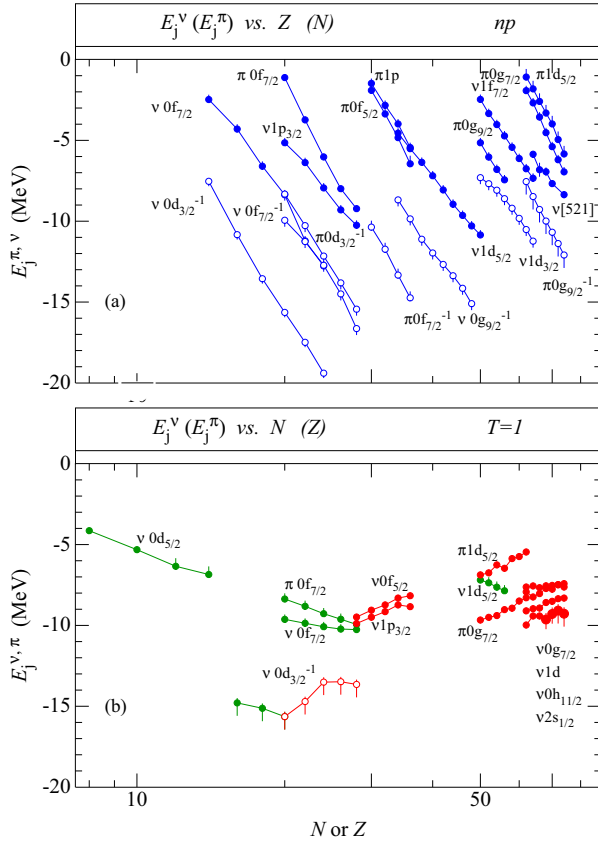
―――――――
*schiffer@anl.gov

FIG. 1. Effective energies ($E_j^{\pi,\nu}$) plotted in terms of absolute binding energies on the target as a function of the changing number of protons or neutrons. The points corresponding to one state are connected by lines. Each segment is labeled as to the configuration of the state studied. Data from purely hole states are open circles, others are filled symbols. In (a), the changing nucleons are of the other kind to the state tracked (*np* interaction) and in (b), the changing nucleons are the same kind as in the state studied (the interaction is $T = 1$) segments where *only* the occupancy of the state in question is changing are shown in green; those where occupancies are changing in several orbitals for the segment are in red. For the data in panel (b) an approximate Coulomb correction is applied to the proton states.

As an example, the first segment on the left of the upper panel of Fig. 1, the hollow points correspond to the energies of the $0d_{3/2}$ neutron-hole excitations in $N = 20$ nuclei, in ^{34}Si, ^{36}S, ^{38}Ar, ^{40}Ca, ^{42}Ti, and ^{44}Cr. There are reaction data available for all but the last two points, where assumptions were made, and the isobaric analog state has to be considered in ^{37}Ar. Some of such details are discussed in the Supplemental Material [21].

In the simple cases, where there is a single neutron or proton (or hole) on a closed shell of the same type of nucleon, and the other type of nucleon is varied, the nucleon-adding or removing strength is often concentrated in one state. Where details of nuclear structure may be more complicated, and the s.p. degree of freedom is fragmented, the spectroscopic-factor weighted centroid energies are taken [26]. Hole states are treated on the same basis as particle states. The energies

are with respect to zero binding of the nucleon or hole, thus always negative.

These segments in Fig. 1(a) are approximately parallel and moving downward, becoming more bound, with added nucleons. The horizontal scale is logarithmic. Where measured, the segments for particle and hole states are almost contiguous. Some of the minor variations in slope are caused by the specific j dependence of the tensor force, that was investigated extensively in connection with changing shell structure [5].

Figure 1(b) shows the data, where the *same* species of nucleons are varied as the states tracked; the values for $E_j^{\pi,\nu}$ are derived by combining the energies of particle and hole excitations, taken as the energy centroids of the nucleon-adding and -removing strengths as defined by Baranger [27]: $E_j^{\pi,\nu} = E_j^+ G_j^+ + E_j^- G_j^-$. Here $E_j^\pm$ are the centroid energies for adding or removing a nucleon, and $G^\pm$ are the summed strengths, with $G_j^+ + G_j^- = 1.0$.

The Baranger expression for combining particle and hole energies is needed when the nucleons varying are of the same species as that of the state studied, and their occupancy is changing, but it is trivially correct even for pure particle or pure hole states. When the occupancy is changing within the string studied, it may be changing either along with those for other orbitals, as in the strings of Ni or Sn isotopes for neutron states when N is changing, or *only* the occupancy of that orbital, as for $\nu 0f_{7/2}$ in the Ca isotopes.

The slopes of all these segments in Fig. 1(b) are much less steep than those in Fig. 1(a), and are shown in different colors, depending on whether only nucleons in the same orbit as the state followed are changing, or the occupancies of several are changing. They are clearly different.

In some cases given in Fig. 1, no transfer reaction data are available, and so simple approximations are made, such as that the final state in question is a single-particle state (sometimes supported by $\log ft$ values or systematics in neighboring nuclei. Errors bars are modified accordingly (and it is noted in Ref. [21].)

There are some concerns as to whether the derived energies are true "observables," particularly when the strength is fragmented, and because of the uncertainties in reaction theory [28,29]. Detailed past works in a few cases [30,31] suggest that the uncertainties from fragmentation are mostly smaller than the change between adjacent points in the segments in Fig. 1. The use of reaction models in determining centroids of single-particle strength also introduces some uncertainties, but these are generally small compared to other contributions to the error bars. We note that for a segment for a given j, in Fig. 1, the Q-value dependence of the calculated cross section (typically done in a distorted wave Born approximation framework) is small, and mostly the spectroscopic-factor weighted energies (centroids) are the same within the error bars, as the cross-section-weighted energies.

The slopes of *all* these segments in Fig. 1(b) are much less steep, by about a factor of four, than those in Fig. 1(a). Here, different colors are used, depending on whether only nucleons in the same orbit as the state tracked are changing, as for $\nu 0f_{7/2}$ in the Ca isotopes, or the occupancies of several orbits are changing as in Ni or Sn isotopes. The slopes for

TABLE I. The logarithmic derivative of the $E_j^{\pi,\nu}$ with respect to nucleon number.

Slope	$dE_j^{\pi,\nu}/d(\ln N)$ (MeV)
Average (*np*)	−21.3 (3.7)
Average ($T = 1$), one orbit	−4.1 (1.3)
Average ($T = 1$), several orbits	+4.6 (1.5)

these two categories are distinctly different. The mean values of the slopes and their rms spread are listed in Table I.

Because the segments shown in Fig. 1(b) involve one type of nucleon, only the $T = 1$ interaction can play a role in the data. An approximate correction to remove Coulomb effects [21] was applied to the cases where Z is changing for proton states to allow a meaningful comparison between neutron and proton data, but higher-order Coulomb effects (e.g., changing radius because of added nucleons) are complex, and no corrections were made.

In one case in Fig. 1(b), the neutron $0d_{3/2}$ holes in the Ca isotopes, the sequence of energies shows a break at $N = 20$, where this orbit is filled. The sequence is split at the shell closure, the data below $N = 20$ are separated from the data above. While the $0d_{3/2}$ orbit is filling, the slope shows the characteristic downward trend, as in all the cases where only the orbit considered is changing its occupancy. Above $N = 20$, as the $0f_{7/2}$ orbit fills, the slope is upward, as is always the case when the occupancy of more than the state studied is changing.

From Fig. 1(a) it is clear that the influence of added neutrons on proton states, or of added protons on neutron states is strongly attractive. This feature has been recognized for a long time Yukawa [32] and is inherent in the nature of pion exchange. An "asymmetry term" is part of the semi-empirical mass formula [33,34]. But our purpose here is not to review the history of the NN interaction.

It is well known and expected from one-pion exchange, that the np and $T = 0$ interactions are much stronger than the $T = 1$.[1] The mean values of the slopes (logarithmic derivative with respect to nucleon number) in the various subgroups and the rms variation among them are shown in Table I. The individual values for these are given in the Supplemental Material [21].

The relative constancy of the slopes in Fig. 1 and Table I over an almost order of magnitude change in nucleon number, has not been explicitly noted before, though it may have been implicitly assumed.

This apparent similarity between the slopes of energies changing with nucleon number, is a feature of plotting them on a logarithmic scale in N or Z. The pattern would be quite different, were the data plotted on a linear scale. The slope for each segment, $d(E_j^{\pi,\nu})/dN$ or dZ, is plotted in Fig. 2. The lines correspond to constant change in energy for the

---

[1] Another reflection of a larger role for the np interaction is in two-nucleon knockout $(e, e'2N)$, where closely correlated np pairs are found to be at least six times more likely than nn and pp pairs [35].
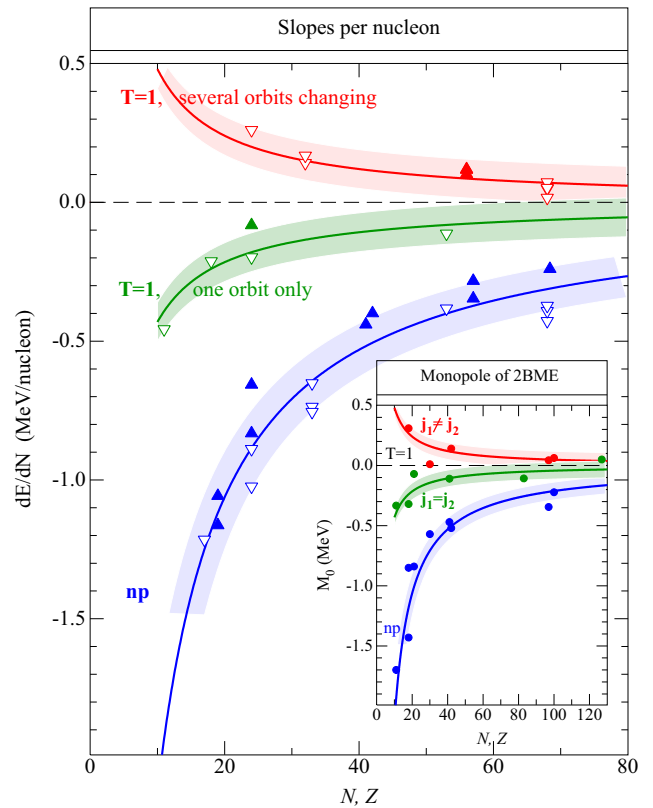

FIG. 2. The slope of effective energies vs nucleon number for the line segments shown in Fig. 1. Blue dots are the slopes for segments where the nucleons changing are different from the one in the state, *np*, those in Fig. 1(a). The red and green points correspond to the slopes of segments where the nucleons are the same species as in the state, $T = 1$, from Fig. 1(b). The lines represent a $1/N$ or $1/Z$ dependence, normalized to the data (the assumption that the slope in fractional change in the numbers of nucleons is constant). The shaded areas indicate the approximate range of the data. The inset shows the monopole of the empirical two-body matrix elements from Ref. [36] as discussed in the text with the nucleon numbers the average of the species contributing to that multiplet for that nucleon. The shaded areas and the lines are the same in the inset as in the main figure.

same *fractional* change in nucleon number, consistent with the naive picture that each nucleon contributes equally to the overall binding field.

Indeed, the slopes of the different line segments follow the lines with some scatter, likely from differences in overlaps between orbits and the details of the effective interaction, such as the tensor component. But the scatter is small compared to the magnitude of the slopes.

The most dramatic difference, evident in Fig. 1 and Table I, is that where the changing nucleons are the same as the one tracked ($T = 1$), the slope is less in absolute magnitude than for the np case. The magnitude of this difference is approximately consistent with the empirical "symmetry term" in the semiempirical mass formula and the Woods Saxon potentials of the optical model for nucleons which is briefly discussed further below.

In a past survey, some of us studied two-nucleon spectra outside closed shells [36], where complete multiplets for two nucleons outside doubly-closed-shell nuclei were reviewed. At doubly closed shells, such as ^{16}O, ^{40}Ca, ^{90}Zr, or ^{208}Pb, where the difference in binding energies of one particle outside the core nucleus is compared with that of the two nucleons, yielding the complete multiplet for the two-body (NN) interaction in nuclei such as ^{210}Bi, ^{210}Pb, and ^{208}Bi.

The monopole moment M_0 of the experimental multiplets should be closely linked to (effectively the same as) the slopes derived here. This is shown in the inset of Fig. 2. The energy in each data point in this inset is the monopole moment of a multiplet from Ref. [36], with the nucleon number the average of that for the two-nucleon species contributing. The process of going from the binding energy of one nucleon to that of two nucleons outside the core, amounts to a two-point segment, and provides a slope in the same sense as used for the data in Fig. 1.

It is remarkable that the M_0 values for identical orbits fall mostly below 0, and the ones for nonidentical ones (red) above it. Thus the observed patterns in the slopes is confirmed, and not an artifice arising from the approximations of the Baranger interpolation [27], for instance. We will return to this briefly below.

The purpose of this note was primarily to present the data with as little reference to models as possible. Nevertheless, some discussion of the potential for the nucleon-nucleus interaction seems appropriate. This was approximated in shell-model studies of nuclear structure by infinite oscillator potentials for the sake of calculational convenience. More recently, *ab initio* calculations have been used to great effect, where the interaction is finite, derived from the free NN scattering, and there are no constraints on radii.

Nucleon-nucleus scattering was parametrized historically since the introduction of the empirical optical model [37], to fit data on the scattering of nucleons on nuclei (for example, Ref. [38]) and later, these finite potentials, were also used to describe bound single-particle states adjacent to closed shells [39]. In Bohr and Mottelson [40] the dependence of single-particle states is shown as a function of A, calculated from an empirical Woods-Saxon potential, and the qualitative agreement with data is mentioned.

As shown in Fig. 3, a pattern qualitatively similar to that seen in the data requires a cancelation between the effect of the symmetry term and the changing radius. A symmetry term with a fixed radius would yield a dependence with slopes that are roughly equal and opposite, while a changing radius with no symmetry term would give essentially the same slopes. But when both are included, the pattern is similar to what is seen in the data. The functional Woods-Saxon form has a diffuse edge and finite binding, and is characterized by a radius that varies as $r_0 A^{1/3}$ and a strength that is a constant, V_0, plus a symmetry term proportional to $\pm V_{sym}(N - Z)/A$. The exact parameters do not matter for this qualitative behavior, the values used were $r_0 = 1.17$ fm, $V_0 = -50$ MeV, and $V_{sym} = 30$ MeV.

The near cancelation of the effects of an increasing radius and a decreasing potential strength happens in the potential for neutrons with changing neutron number. But in the proton potential the radius still increases, but the sign of the
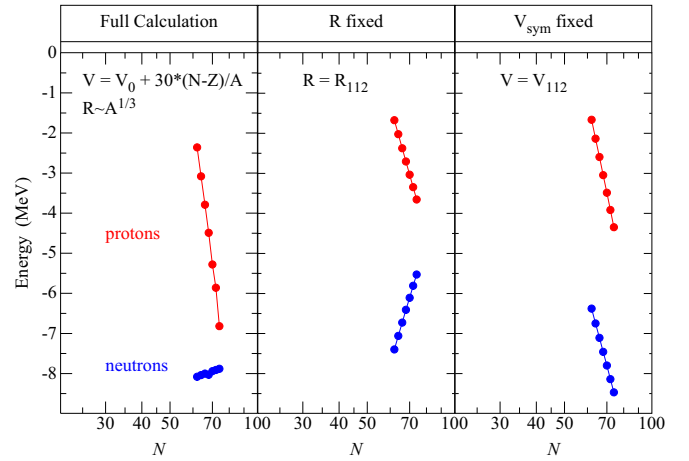

FIG. 3. Calculations of the changing energy of a $1/2^+$ state in a Woods-Saxon potential for the seven stable even Sn isotopes. The red points show the behavior of a proton state, the blue ones for a neutron state. The left panel shows the behavior with neutron number N with a typical potential, radius increasing as $A^{1/3}$ and a symmetry term proportional to $(N - Z)/A$. The middle panel shows the results with the same symmetry term and the radius fixed at that for ^{112}Sn. The right-hand panel is with no $(N - Z)/A$ dependence, the potential fixed at the value for ^{112}Sn, and the radius again changing as $A^{1/3}$.

symmetry-term contribution to the potential changes, the two terms have the same sign, and reinforce the change. That is as should be expected with an empirical potential.

One should not regard this as an "explanation," rather that the empirical parametrization does describe the data, reasonably well. The symmetry term implicitly assumes that it is a perturbation on the main part of the interaction. But in view of the trend in the data that the interaction of a neutron, with another neutron is different from that with a proton, it is tempting to write a mathematically exactly equivalent form in terms of a first term describing the interaction with the other type of nucleons V_{np}, and the second with the same type, $V_{T=1}$ instead of V_0 and V_{sym}, as we have done in Eq. S2 in the Supplemental Material [21]. This would yield $V_{np} \cong -80$ MeV and $V_{T=1} \cong -20$ MeV (and thus, $V_{T=0} \cong -140$).

The observation that the $T = 0$ and "np" interactions are much stronger than that between identical $T = 1$ nucleon pairs is certainly not new. Nor is the fact that, on average, the nuclear radius changes as $A^{1/3}$. The interaction between the increasing radius and the symmetry term, is built into the empirical parametrization of the Woods-Saxon potential. Consider the string of Sn isotopes with 50 protons. These protons are the dominant source of the potential that binds the neutrons. The closed shell of protons remains essentially the same throughout the Sn isotopes, except that the nuclei must be getting larger with added neutrons and the protons spread out over a larger volume. If these protons all contribute equally to the overall potential, then their dilution will correspond to a weaker potential, and this effect must be incorporated in the symmetry potential. This qualitative argument needs to be taken with caution, because the measured charge radius is changing in a somewhat complex way; at a rate slower than $A^{1/3}$ when neutrons are added, but the rate is not the same in

the Sn isotopes as in the Ca isotopes. The use of the symmetry term in the average potential is a useful empirical tool, but it is an approximation.

This may perhaps help to suggest an explanation for the two groups of slopes for the $T = 1$ segments In Figs. 1 and 2. The behavior of the corresponding two-body matrix elements from Ref. [36] are shown in the inset of Fig. 2. As was already noted the behavior of the two groups of $T = 1$ slopes is very similar to the pattern of $T = 1$ matrix elements in [36] for the $j_1 = j_2$ and the $j_1 \neq j_2$ matrix elements. In that reference, the very small (and sometimes repulsive) monopole matrix elements were approximately reproduced by two interactions, an attractive Yukawa potential with a range of one-pion exchange, and a longer range repulsive term, that tended to cancel the average attraction; the fit was not sensitive to the exact range of the repulsive term as long as it was longer than that of the attractive one. The need and magnitude of the attraction was determined by the higher multipole content (downward curvature) of the two-body spectra; in particular see the behavior of the $T = 1$ matrix elements in Figs. 2 and 6 of Ref. [36].

In re-examining the details of that cancelation, it seems that, on the average, the attractive term is slightly larger (by a few percent) when the two nucleons are in the same orbit, than when they are in different orbits, as may be expected because of a more perfect radial overlap. The data requires a near-zero monopole term. In Ref. [36], oscillator wave functions were used without allowing for a changing radius between, for instance, ^{41}Ca and ^{42}Ca. Using crude arguments, the magnitude of this effect of a changing radius is comparable to making the monopole interaction slightly repulsive.

In retrospect, and in view of the behavior with radius shown in Fig. 3, one may wonder whether the apparent repulsive term may have its origin in the effect of the inevitably changing radius, that is traditionally ignored. But our purpose here is to point out trends in the data, and leave it to further work to come up with possible model explanations for the simple trends that are apparent in the largely model-independent features.

To summarize, our survey of the data indicates at least four features, three of which were apparently not fully recognized, and that may help as a guide to our intuition, beyond what seems to be generally understood and accepted.

(1) The change in single-particle energies with nucleon number is qualitatively different, depending on whether the nucleons in the state are the same or different from those changing.

(2) The change per nucleon, is essentially the same as the experimentally observed monopole term in the effective NN interaction.

(3) The change with *fractional* change in nucleon number is remarkably constant from $A \approx 16$ to almost 208.

(4) For identical nucleons, the change is small, but it *does* matter whether the nucleons are all in the same orbit or not. The change in radius between adjacent nuclei seems to have a significant influence on the effective interaction, particularly between identical nucleons.

As the field moves toward more and more exotic nuclei, near the limits of binding, and the quality of data improves, the question of how the binding energies of individual orbits change with added nucleons, and exploring and understanding systematics is likely to help complement the detailed work on the evolution of shell structure.

[1] M. G. Mayer, Phys. Rev. **75**, 1969 (1949).

[2] O. Haxel, J. H. D. Jensen, and H. E. Suess, Phys. Rev. **75**, 1766 (1949).

[3] O. Sorlin and M.-G. Porquet, Prog. Part. Nucl. Phys. **61**, 602 (2008).

[4] T. Otsuka, A. Gade, O. Sorlin, T. Suzuki, and Y. Utsuno, Rev. Mod. Phys. **92**, 015002 (2020).

[5] T. Otsuka, T. Suzuki, R. Fujimoto, H. Grawe, and Y. Akaishi, Phys. Rev. Lett. **95**, 232502 (2005).

[6] T. Otsuka, T. Suzuki, J. D. Holt, A. Schwenk, and Y. Akaishi, Phys. Rev. Lett. **105**, 032501 (2010).

[7] A. Cipollone, C. Barbieri, and P. Navrátil, Phys. Rev. C **92**, 014306 (2015).

[8] A. Poves and A. Zuker, Phys. Rep. **70**, 235 (1981).

[9] T. Otsuka, T. Suzuki, M. Honma, Y. Utsuno, N. Tsunoda, K. Tsukiyama, and M. Hjorth-Jensen, Phys. Rev. Lett. **104**, 012501 (2010).

[10] J. P. Schiffer, S. J. Freeman, J. A. Caggiano, C. Deibel, A. Heinz, C.-L. Jiang, R. Lewis, A. Parikh, P. D. Parker, K. E. Rehm, S. Sinha, and J. S. Thomas, Phys. Rev. Lett. **92**, 162501 (2004).

[11] S. V. Szwec, D. K. Sharp, B. P. Kay, S. J. Freeman, J. P. Schiffer, P. Adsley, C. Binnersley, N. de Séréville, T. Faestermann, R. F. Garcia Ruiz, F. Hammache, R. Hertenberger, A. Meyer, C. Portail, I. Stefan, A. Vernon, S. Wilkins, and H.-F. Wirth, Phys. Rev. C **104**, 054308 (2021).

[12] Binding energies from nuclear masses; see, for example, W. J. Huang, M. Wang, F. G. Kondev, G. Audi, and S. Naimi, Chinese Phys. C **45**, 030002 (2021); M. Wang, W. J. Huang, F. G. Kondev, G. Audi, and S. Naimi, *ibid.* **45**, 030003 (2021).

[13] B. L. Cohen, Rev. Mod. Phys. **35**, 332 (1963).

[14] R. K. Bansal and J. B. French, Phys. Lett. **11**, 145 (1964); **19**, 223 (1965).

[15] National Nuclear Data Center, information extracted from the Evaluated Nuclear Structure Data File (ENSDF)), https://www.nndc.bnl.gov/ensdf/ and the Experimental Unevaluated Nuclear Data List (XUNDL), https://www.nndc.bnl.gov/ensdf/.

[16] B. H. Wildenthal, E. Newman, and R. L. Auble, Phys. Rev. C **3**, 1199 (1971).

[17] S. S. Ipson, W. Booth, and J. G. B. Haigh, Nucl. Phys. A **206**, 114 (1973).

[18] W. Booth, S. Wilson, and S. S. Ipson, Nucl. Phys. A **238**, 301 (1975).

[19] J. P. Schiffer, C. R. Hoffman, B. P. Kay, J. A. Clark, C. M. Deibel, S. J. Freeman, M. Honma, A. M. Howard, A. J. Mitchell, T. Otsuka, P. D. Parker, D. K. Sharp, and J. S. Thomas, Phys. Rev. C **87**, 034306 (2013).

[20] D. K. Sharp, B. P. Kay, J. S. Thomas, S. J. Freeman, J. P. Schiffer, B. B. Back, S. Bedoor, T. Bloxham, J. A. Clark, C. M. Deibel, C. R. Hoffman, A. M. Howard, J. C. Lighthall, S. T. Marley, A. J. Mitchell, T. Otsuka, P. D. Parker, K. E. Rehm, D. V. Shetty, and A. H. Wuosmaa, Phys. Rev. C **87**, 014312 (2013).

[21] See Supplemental Material at http://link.aps.org/supplemental/10.1103/PhysRevC.105.L041302 for information on the data used, which includes Refs. [22,23].

[22] K. L. Jones, A. S. Adekola, D. W. Bardayan, J. C. Blackmon, K. Y. Chae, K. A. Chipps, J. A. Cizewski, L. Erikson, C. Harlin, R. Hatarik, R. Kapler, R. L. Kozub, J. F. Liang, R. Livesay, Z. Ma, B. H. Moazen, C. D. Nesaraja, F. M. Nunes, S. D. Pain, N. P. Patterson, J. F. Shriner Jr. *et al.*, Nature (London) **465**, 454 (2010).

[23] I. Angeli and K. P. Marinova, At. Data Nucl. Data Tables **99**, 69 (2013).

[24] B. Elbek and P. O. Tjøm, in *Advances in Nuclear Physics*, edited by M. Baranger and E. Vogt, Vol. 3 (Plenum Press, New York, 1969).

[25] B. P. Kay, J. P. Schiffer, S. J. Freeman, T. L. Tang, B. D. Cropper, T. Faestermann, R. Hertenberger, J. M. Keatings, P. T. MacGregor, J. F. Smith, and H.-F. Wirth, Phys. Rev. C **103**, 024319 (2021).

[26] J. B. French, in *Proceedings of International School of Physics Enrico Fermi, Course 36, Varenna 1965*, edited by C. Bloch (Academic Press, New York, 1966), p. 278.

[27] M. Baranger, Nucl. Phys. A **149**, 225 (1970).

[28] J. P. Schiffer, C. R. Hoffman, B. P. Kay, J. A. Clark, C. M. Deibel, S. J. Freeman, A. M. Howard, A. J. Mitchell, P. D. Parker, D. K. Sharp, and J. S. Thomas, Phys. Rev. Lett. **108**, 022501 (2012).

[29] S. J. Freeman, D. K. Sharp, S. A. McAllister, B. P. Kay, C. M. Deibel, T. Faestermann, R. Hertenberger, A. J. Mitchell, J. P. Schiffer, S. V. Szwec, J. S. Thomas, and H.-F. Wirth, Phys. Rev. C **96**, 054325 (2017).

[30] T. Duguet and G. Hagen, Phys. Rev. C **85**, 034330 (2012).

[31] T. Duguet, H. Hergert, J. D. Holt, and V. Somà, Phys. Rev. C **92**, 034313 (2015).

[32] H. Yukawa, Proc. Phys. Math. Soc. Jpn. **17**, 48 (1935).

[33] C. F. v. Weizsäcker, Z. Phys. **96**, 431 (1935).

[34] H. A. Bethe and R. F. Bacher, Rev. Mod. Phys. **8**, 82 (1936).

[35] E. Piasetzky, M. Sargsian, L. Frankfurt, M. Strikman, and J. W. Watson, Phys. Rev. Lett. **97**, 162504 (2006).

[36] J. P. Schiffer and W. W. True, Rev. Mod. Phys. **48**, 191 (1976).

[37] H. Feshbach, C. E. Porter, and V. F. Weisskopf, Phys. Rev. **96**, 448 (1954).

[38] A. J. Koning and J. P. Delaroche, Nucl. Phys. A **713**, 231 (2003).

[39] N. Schwierz, I. Wiendenhöver, and A. Volya, arXiv:0709.3525.

[40] A. Bohr and B. R. Mottelson, *Nuclear Structure*, Vol. 1 (W. A. Benjamin, New York, 1969).